Journal of the Arkansas Academy of Science

Volume 66 Article 8

2012

Fabrication and Characterization of Aluminum-doped ZnO/PANI Hybrid Solar Cells

S. AbdulAlmohsin
University of Arkansas at Little Rock, samir_mahdi47@yahoo.com

S. M. Al-Mutoki
Technical Institute Of Shatrah

Z. Li
University of Arkansas at Little Rock

Recommended Citation

AbdulAlmohsin, S.; Al-Mutoki, S. M.; and Li, Z. (2012) "Fabrication and Characterization of Aluminum-doped ZnO/PANI Hybrid Solar Cells," *Journal of the Arkansas Academy of Science*: Vol. 66 , Article 8.
DOI: https://doi.org/10.54119/jaas.2012.6601
Available at: https://scholarworks.uark.edu/jaas/vol66/iss1/8

Fabrication and Characterization of Aluminum-doped ZnO/PANI Hybrid Solar Cells

S. AbdulAlmohsin[1*], S.M. AL-Mutoki[2] and Z. Li[1]

[1]*Department of Physics, University of Arkansas, Little Rock, AR 72204,USA*
[2]*Electrical Department, Foundation Of Technical Education, Technical Institute Of Shatrah,Shatrah, ThiQar00964, Iraq*

*Correspondence: samir_mahdi47@yahoo.com

Abstract

We report a facile method to fabricate an AZO/PANI heterostructure by a sandwiching technique. Aluminum-doped ZnO (AZO) films were deposited onto indium tin oxide (ITO) glass using the sputtering technique while PANI films were deposited onto ITO glass using electropolymerization. The optoelectric properties of the inorganic/organic device were characterized.

Introduction

Transparent conductive oxides (TCOs) have a wide range of applications in many fields such as gas sensors (Gupta et al. 2010), piezoelectric (Lorenz-Hallenberg 2003), solar cells (Sittinger et al. 2008) and as transparent conductive electrodes (Shi et al. 2000). TCOs have unique properties that combine both high transparency and high conductivity. In the majority of semiconductors, conductivity and transparency are repulsive and oppose each other. In TCOs, the large band gap (≈ 3.4 eV) makes them transparent to the region of interest in the solar applications and the non-stoichiometry (lack of oxygen) results in high free charge concentration and then high conductivity. Indium tin oxide (ITO) is widely and commercially used as TCO material, but indium is a scarce element on Earth, and is toxic. Another drawback of ITO is that it has low chemical stability. Aluminum-doped zinc oxide (AZO) has attracted increasing interest over the years and has been investigated as an alternative to ITO because it exhibits high transmittance (> 90%) and low resistivity (around 10^{-4} Ohm.cm) (Jin et al. 1993). AZO is supposed to be less expensive than ITO and also less toxic. As with any TCO materials, AZO is an n-type semiconductor in nature, with a bandgap around 3.4 eV (Jung et al. 2009). AZO films can be prepared by different methods, such as spray pyrolysis (Kaid et al. 2007), and sputtering (Kong et al. 2011). Sputtering is a common way to deposit AZO by using ZnO and Al_2O_3 targets and sometimes by using two separate targets of Al and ZnO (Fenske et al. 1999). Recently, AZO nanoparticles (NPs) have attracted increasing attention (Benouis et al. 2007) as a result of the rapid development of nanotechnology and nanomaterials. One of the promising applications of AZO NPs is the production of efficient solar converters because the NPs films introduce a large junction area in solar cells.

Polyaniline (PANI) is one of the best, facile and conductive polymers (Rimbu et al. 2006) with feasible stability against the environment (Ansari et al. 2006). Its conductivity arises from the π-electron conjugate in the polymeric chain. PANI is naturally a p-type material with an optical band gap of about 3 eV. As a polymer, the energy gap diagram of PANI is not comprised of conduction and valence bands, but rather it is described by the highest occupied molecular orbital (HOMO) and the lowest unoccupied molecular orbital (LUMO). The HOMO level of PANI is 7.7 eV, while the LOMO level is 4.7 eV. (Catedral et al. 2004). PANI can be synthesized by different techniques, such as plasma enhanced polymerization (Sadia et al. 2009) and electrochemical techniques (Martinez et al. 2008).

Recently, hybrid inorganic/organic heterojunction devices have received much attention as promising junctions for many applications, such as gas sensors (Gong et al. 2010), light emitting diodes (He et al. 2010), and photo detectors (Mahmoud 2009). ZnO/PANI has gained a lot of interest for its luminescence properties (Amrithesh et al. 2009) and UV detection (Moreira et al. 2009). In this paper, AZO/PANI heterostructure sandwiched between two ITO-coated glass was studied. AZO films were deposited using the sputtering technique while PANI films were deposited using by electro polymerization. The AZO films in solar cells are used as a window layer and an active material.

Methods

Aniline monomer was distilled twice under reduced pressure before use, and dissolved into a 1 M sulfuric acid to make a 0.1 M solution. The polyaniline was synthesized with a galvanostatic step method at a constant voltage of 3 V. The working electrode was a

commercial ITO-glass with a surface area of 1.5 cm^2. A paper clip was used as a counter electrode. The amount of the electrodeposited polyaniline was estimated by weighing the working electrode before and after the electro deposition. Figure 1 displays a schematic diagram of the electrochemical cell for in situ polymerization.

The AZO film was sputtered onto the ITO glass with sputtering power of 150 W under Ar pressure in the range 24 mtorr ~ 30 mtorr with a flow rate of 0.075 to 0.076 ml/min. An ZnO disk with 2 wt% Al_2O_3 impurity was used an anode. The substrate temperature was kept at 180 ^oC, the current was set at 0.097 to 0.101 A, and voltage of 261 to 202 V, with a sputter time of 40 min.

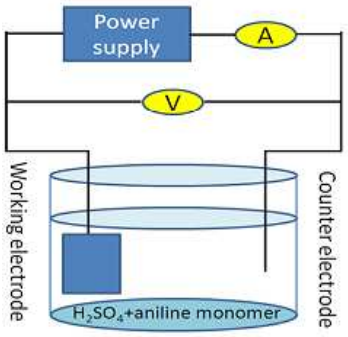

Figure 1. Schematic diagram of the electrochemical cell used to prepare the PANI thin film.

AZO film and PANI were brought into contact by sandwiching them to create the heterostructure. To ensure intimate contact between the AZO and the PANI, the two films were sandwiched right after the electrochemical process when the PANI was still wet. A schematic diagram of the fabricated device is illustrated in Figure 2. Current density-voltage (J-V) characteristics have been investigated in the dark and under illumination using an AM1.5 sunlight simulator. Irradiation was achieved from the TiO_2 side and from the nanocomposite side.

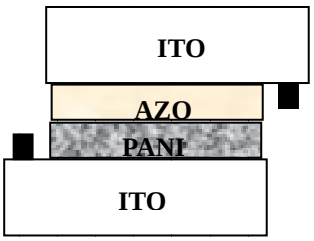

Figure 2. A schematic diagram of the AZO-PANI heterostructure.

Results and Discussion

Figure 3 demonstrates the surface topography of AZO NPs using the scanning electron microscopy (SEM). The diameter of AZO NPs ranges from 50 nm to 100 nm. The film displays a good uniformity with little agglomeration.

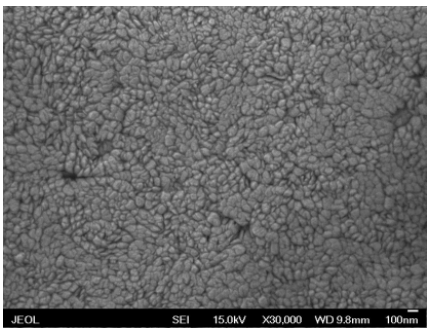

Figure 3. SEM photo of AZO NPs deposited onto ITO glass.

The dark J-V characteristics of the AZO/PANI heterodiode shown in Figure 4 exhibit a rectifying behavior with a rectification of 28 at ±1 V (rectification stands for the ratio of the forward to reverse current at a certain bias voltage). The rectifying behavior indicates the formation of a diode between AZO n-type film and PANI p-type film. The reverse current of this diode illustrates a gradual increase, referring to a soft break-down, which is a feature of the heterojunction diode. The forward current shows an exponential behavior of the form:

$$\mathbf{I = I_o \exp\left(\frac{qV}{nkT}\right)} \quad , \qquad \mathbf{(1)}$$

where I_o is the saturation current, V is the bias voltage, q/kT is the thermal energy and n is the ideality factor. Figure 5 represents the semi-log I-V curve of the device. The curve exhibits a linear behavior in the bias region of 0.05-0.3 V. The empirical equation of this diode is:

$$\mathbf{I = 0.00004\exp(8.87V)} \qquad \mathbf{(2)}$$

The equation indicates an extrapolated saturation current of 4 × 10^{-5} A, while the ideality factor that is calculated from this equation is 4.3. The high value of n suggests that the carrier transport of this device is dominated by more than one mechanism.

https://scholarworks.uark.edu/jaas/vol66/iss1/8
DOI: https://doi.org/10.54119/jaas.2012.6601

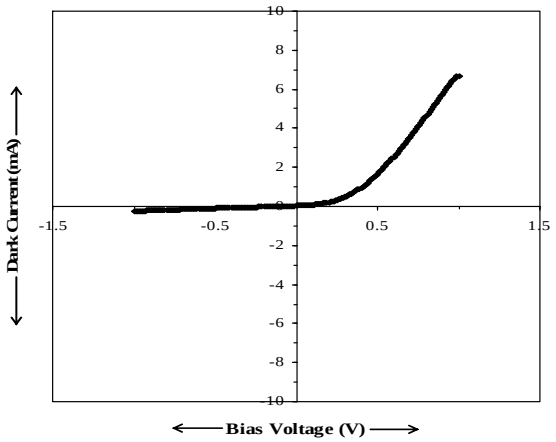

Figure 4. Dark I-V characteristics of AZO/PANI heterojunction, y-axis multiply by 10^{-2}.

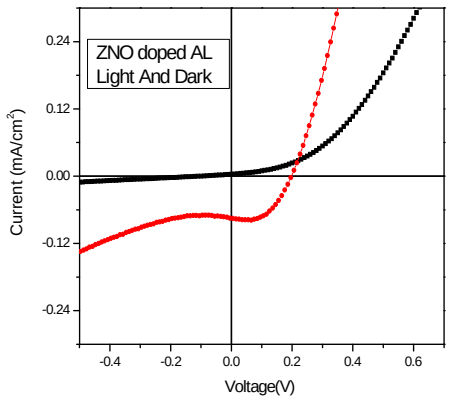

Figure 6. The J-V characteristics under AM1.5 illumination.

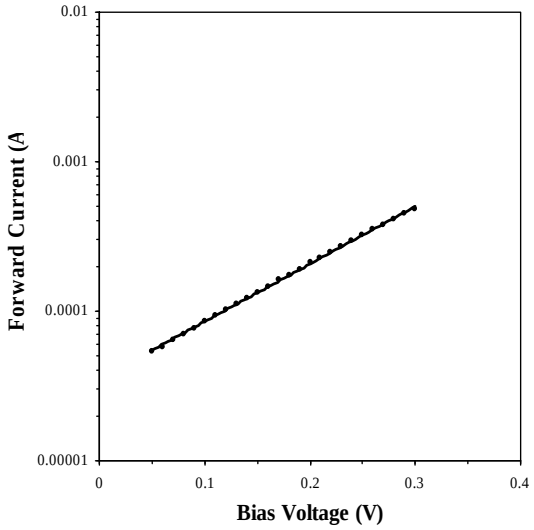

Figure 5. The semi-log I-V plot at the forward bias, Y-Axes multiply by 10^{-2}.

The J-V characteristics of the AZO/PANI thin film solar cell exhibit considerable photovoltaic performance under illumination AM 1.5 (~100 mW/cm^2), as depicted in Fig. 6, with a short circuit current density (I_{SC}) of 0.075 mA/cm^2, an open circuit voltage (V_{OC}) of 195 V and a fill-factor (FF) of 0.41. The photon conversion efficiency (PCE) of the cell is 0.0078%, which indicates a significant performance.

The photovoltaic performances of the AZO/PANI devices under different illumination intensities are listed in Table 1.

The use of the sandwiching technique to fabricate a heterojunction has not been reported in the literature to date and most of the existing papers use the subsequent deposition of the two layers. The rectification behavior and the acceptable photovoltaic performance of the device presented above suggest a successful formation of a heterojunction between AZO nanoparticles and PANI, indicating that the sandwiching technique is useful in the fabrication of this kind of heterojunction. The wet surface of PANI directly after the electropolymerization helps to form an intimate contact with AZO nanoparticle film, and the morphology of the bumpy AZO surface could help to increase the junction area. An SEM photographs. In the subsequent deposition, the AZO nanoparticle film needs to be used as a working electrode. That can cause a degradation of the AZO film when it is immersed in the electrolyte and, in addition, the AZO film may dissolve in the electrolyte because of the effect of the sulfuric acid. Furthermore, the subsequent deposition needs to make ohmic contact onto the PANI surface, requiring the use of the evaporation technique to deposit the metal onto the PANI surface, which could degrade the PANI performance.

Table 1. The photovoltaic performances of the AZO/PANI devices under different illumination intensities.

Illumination (mW/cm^2)	I_{sc} (mA/cm^2)	V_{oc} (volt)	FF	PCE (%)
100	0.075	0.195	0.41	6.0×10^{-3}
80	0.055	0.18	0.57	7.1×10^{-3}
50	0.04	0.15	0.63	7.6×10^{-3}
25	0.025	0.15	0.61	9.1×10^{-3}

The room temperature photoluminescence (PL) of AZO nanoparticles deposited onto ITO glass is shown

Fabrication and Characterization of Aluminum-doped ZnO/PANI Hybrid Solar Cells

in Figure 8. The PL spectrum shows a near-band-edge at 3.46 eV, which represents the direct band gap of AZO. The deep-level emission appears at 2.27 eV, which represents the defects inside the AZO nanoparticles. The intensity ratio ($I_{near\text{-}band}/I_{deep\text{-}level}$) is about 1.8, indicating a very high quality film with high crystallinity and is higher than previously reported results (Kim et al. 2008). The PANI film shows a PL peak of 2.9 eV which is very close to the reported band gap of PANI (Abrarov et al. 2005).

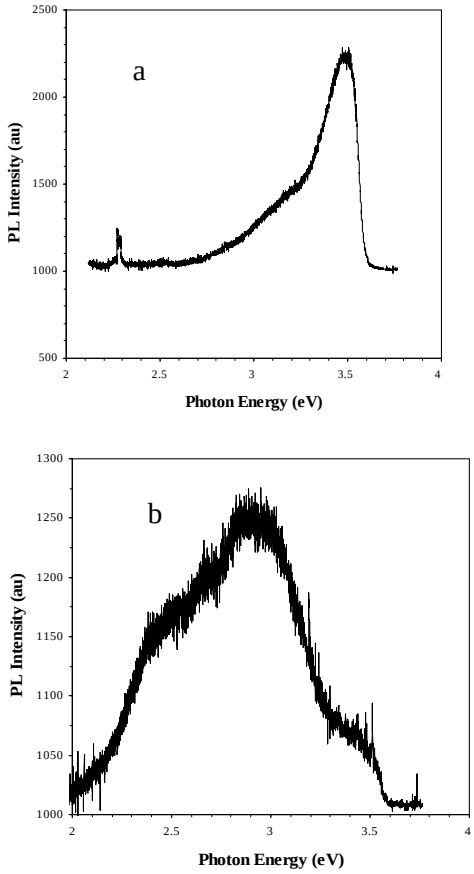

Figure 8. The photoluminescence spectrum of (a) AZO NPs and (b) PANI film.

The optical band gap of AZO film was calculated based on the location of the absorption peak. The band gap for AZO film was 3.2 eV. For AZO films, ions and Al interstitial atoms determines the widening of the band gap caused by increase in carrier concentration. This is the well known Burstein–Moss effect due to the Fermi level moving into the conduction band. According to the Burstein–Moss effect, the broadening of the optical band is a result for doping by Al atoms.

Figure 9 displays the graph of $(\alpha h\nu)^2$ vs.photon energy hν for the AZO thin film obtained by the supterring method. The linear dependence of $(\alpha h\nu)^2$ on hν at higher photon energies indicates that AZO film is essentially direct-transition–type semiconducter. The straight-line portion of the curve, when extrapolated to zero, gives the optical band gap. From the results of Figure 9, optical band gap E_{opt} for AZO thin film is 3.2 eV. This band gap is known as the Moss-Burstein shift.

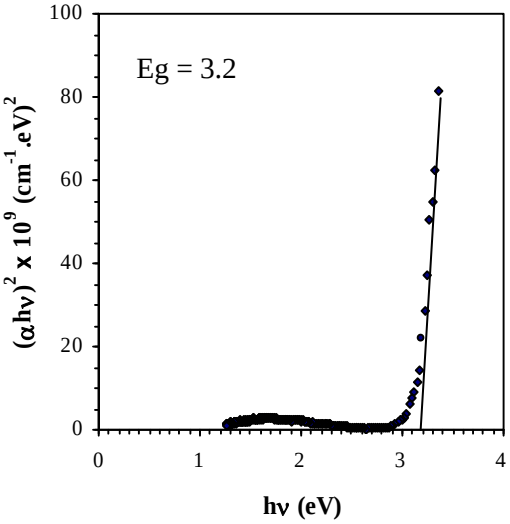

Figure 9. Energy band gap determination of AZO sample at room temperature.

Conclusions

In this manuscript, we report the fabrication of aluminum-doped ZnO (AZO) nanoparticle coating on ITO glass by using sputtering technique and the synthesis of PANI on ITO glass by using electropolymerization. A new type of organic/inorganic hybrid solar cells based on the AZO/PANI heterostructure was developed by sandwiching the two coated ITO glass plates, and the optoelectric properties of devices studied show these heterostructures to be promising organic/inorganic solar cells devices.

Literature Cited

Abrarov SM, **S Yuldashev**, **TW Kim**, **YH Kwon**, and **TW Kang**. 2005. Deep level emission of ZnO nanoparticles deposited inside UV opal. Journal of Luminescence 114:118-124.

Amrithesh M, **S Aravind**, **J Jayalekshmi** and **RS Jayasree**. 2008. Enhanced luminescence observed in polyaniline –polymethylmethacrylate composite. Journal of Alloys and Compounds 449(1-2):176-179.

https://scholarworks.uark.edu/jaas/vol66/iss1/8
DOI: https://doi.org/10.54119/jaas.2012.6601

Ansari R and **MB Keivani**. 2006. Polyaniline conductive electroactive polymers: thermal and environmental stability studies**.** E-Journal of Chemistry 3(4):202-217.

Benouis CE, **AS Juarez** and **MS Aida**. 2007. Physics properties comparison between undoped ZnO and AZO, IZO doped thin films prepared by spray pyrolysis. Journal of Applied Science 7(2):220-225.

Catedral MD, **AKG Tapia**, **RV Sarmago**, **JP Tamayo** and **EJ del Rosario**. 2004. Effect of dopant ions on the electrical conductivity and microstructure of polyaniline (emeraldine salt). Science Diliman 16 (2):41-46.

Fenske F, **W Fuhs**, **E Nebauer**, **A Schöpke**, **B Selle** and **I Sieber**. 1999. Transparent conductive AZO films by reactive co-sputtering from separate metallic Zn and Al Targets. Thin Solid films 343-344:130-133.

Gong J, **Y Li**, **Z Hu**, **Z Zhou** and **Y Deng**. 2010. Ultrasensitive NH_3 gas sensor from polyaniline Nanograin enchased TiO_2 fibers. Journal of Physical Chemistry C 144:9970-9974.

Gupta SK, **A Joshi** and **M Kaur**. 2010. Development of gas sensors using ZnO nanostructures. Journal of Chemical Sciences 122(1):57-62.

He Y, **JA Wang**, **W Zhang**, **J Song**, **C Pei** and **X Chen**. 2010. ZnO-nanowire/PANI inorganic /organic hetrostructure light-emitting diode. Journal of Nanoscience Nanotechnology 10:7254-7.

Jin AJ and **KK Han**. 1993. Low resistance and highly Transparent ITO-Ag-ITO multilayer electrode using surface Plasmon resonance of Ag layer bulk hetrojunction organic solar cells. Solar Energy Materials and Solar Cells 10:1801-1809.

Jung YS, **HW Choi** and **HK Kyung**. 2009. Properties of AZO thin films for solar cells deposited on polycarbonate substrates. Journal of the Korean Physicals Society 55(5):1945-1949.

Kaid MA and **A Ashour**. 2007. Preparation of AZO films by spray pyrolysis technique. Applied Surface Science 253:3029-3033.

Kim JH, **DS Park**, **JH Yu**, **TS Jeong** and **CJ Youn**. 2008. Structural, electrical and optical properties of epitaxial ZnO layers grown with various O_2 flows by radio-frequency magnetron sputtering. Journal of the Korean Physical Society 52:1818-1822.

Kong H, **P Yang** and **J Chu**. 2011. Processing parameters and property of AZO thin film prepared by magnetron sputtering. Journal of Physics: Conference Series 276:12170-12174.

Lorenz-Hallenberg JI. 2003. Application of poly(3,4-ethylenedioxytheophene)-poly(styrenesulfonate) to poly(vinylidene fluoride) as a Replacement for Traditional Electrodes [M.S. Thesis] Montana State University, August.

Mahmoud WE. 2009. A novel photodiode made of hybrid Organic/inorganic nano composite. Journal of Physics D: Applied Physics 42:155502-155506.

Martinez MJ, **C Peng**, **S Zhang** and **G Chen**. 2008. Electrochemical methods enhance the capacitance in activated carbon/polyaniline composite. Journal of Electrochemical Society 155(10):1-7

Moreira LF, **MR Lanza**, **AA Tanka** and **P Sotomayor**. 2009. Selective UV-filter detection with sensors based on stainless steel electrodes modified with polyaniline doped with metal tetrasulfonated phthalocyanine films. Analyst 134:1453-1461.

Rimbu GA, **I Stamatin**, **CL Jackson** and **K Scott**. 2006. The morphology control of polyaniline as conducting polymer in fuel cell technology. Journal of Optoelectronics and Advanced Materials 8(2):670-674.

Sadia A, **SG Ansari**, **M Song**, **YS Kim** and **HS Shin**. 2009. Plasma-enhanced polymerized aniline/TiO_2 dye sensitized solar cells. Super Lattices and Microstructures 46:5-9.

Shi Y, **C Zhang**, **JH Bechtel**, **LR Dalton**, **B Robinson** and **WH Steier**. 2000. Low (sub-1-Volt) half voltage polymeric electro-optic modulators achieved by controlling chromophore shape. Science 288:119-122.

Sittinger V, **F Ruske**, **W Werner**, **C Jacobs**, **B Szyszka** and **DJ Christie**. 2008. High power pulsed magnetron sputtering of transparent conducting oxides. Thin Solid Films 516:5847-5849.